Electronic Supplementary Information

High-throughput large-scale microfluidic assembly of iron oxide magnetite nanoflowers@PS-b-PAA polymeric micelles as multimodal nanoplatforms for photothermia and magnetic imaging

Emilia Benassai[1], Ana C. Hortelao[1], Elif Aygun[2,3], Asli Alpman[2,3], Claire Wilhelm[4], Emine Ulku Saritas[2,3] and Ali Abou-Hassan[1,5]

[1] Sorbonne Université, UMR CNRS 8234, PHysico-chimie des Électrolytes et Nanosystèmes InterfaciauX (PHENIX), F-75005, Paris, France
[2] Department of Electrical and Electronics Engineering, Bilkent University, Ankara, Turkey, 06800
[3] National Magnetic Resonance Research Center (UMRAM), Bilkent University, Ankara, Turkey, 06800
[4] Laboratoire Physico Chimie Curie, PCC, CNRS UMR168, Institut Curie, Sorbonne University, PSL University, Paris, 75005 France
[5] Institut Universitaire de France (IUF), 75231 Cedex 05, Paris, France

Corresponding author: ali.abou_hassan@sorbonne-universite.fr

Table S1. Sample names (capital letters) and respective variable and constant parameters for the continuous flow synthesis of IONF@PS-b-PAA magnetomicelles.

| Sample Names	H_2O Flow (Q_1, Q_2)	THF Flow	Total Flow	τ	α	[Fe] 1:5	[PS-b-PAA] 4:5
	$mL \cdot min^{-1}$	$mL \cdot min^{-1}$	$mL \cdot min^{-1}$	s		$g \cdot L^{-1}$	$g \cdot L^{-1}$
i	10.000	2.857	22.857	1	7	0.2	1.2
ii	7.000	2.000	16.000	2	7	0.2	1.2
iii	4.200	1.200	9.600	3	7	0.2	1.2
iv	2.800	0.800	6.400	4	7	0.2	1.2
v	1.400	0.400	3.200	9	7	0.2	1.2
vi	0.700	0.200	1.600	18	7	0.2	1.2
vii	0.175	0.050	0.400	71	7	0.2	1.2
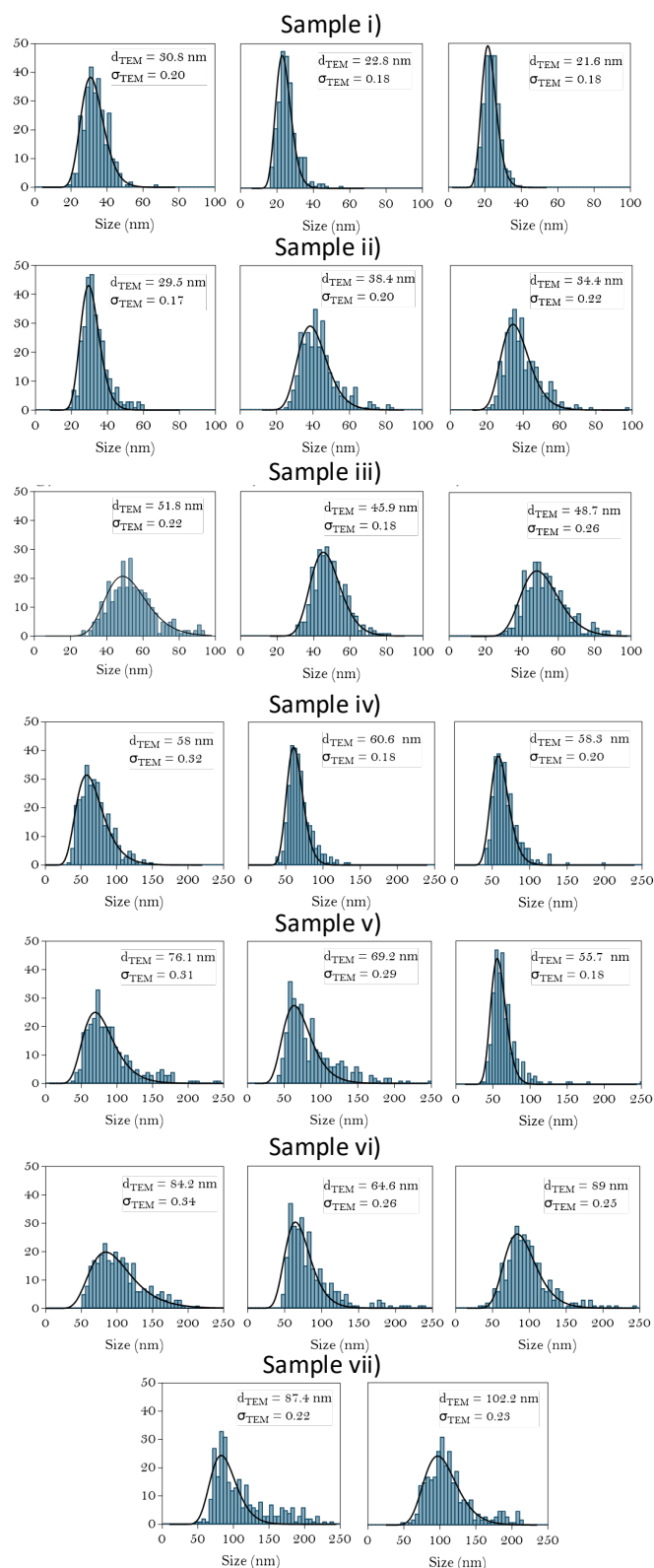
Figure S1. Size distribution histograms of IONF@PS-b-PAA magnetomicelles fitted by a log-normal law and synthetized in triplicate or duplicate of the different magnetomicelles synthesized by modulating the residence time in the microfluidic channel. Black line: log-normal model.

Table S2. Physical diameter (d_{TEM}) and polydispersity (σ_{TEM}) and their averaged values ($\langle d_{TEM}\rangle$, $\langle\sigma_{TEM}\rangle$) of triplicate sharing the same synthesis conditions (as described in Table 9). Hydrodynamic diameters (d_H) and zeta potentials (ζ) obtained by DLS analysis are also reported, along with their averaged values ($\langle d_H\rangle$, $\langle\zeta\rangle$) and the parameter of aggregation δ_{agg}.

Sample Name	d_{TEM}	$\langle d_{TEM}\rangle$	σ	$\langle\sigma\rangle$	d_H	$\langle d_H\rangle$	ζ	$\langle\zeta\rangle$	δ_{agg}
	nm	nm	nm	nm	nm	nm	mV	mV	%
i	31		0.2		20		-26		
	23	25 ($\pm$ 5)	0.18	0.187 ($\pm$ 0.012)	27	26 ($\pm$ 5)	-20	-24 ($\pm$ 4)	3
	22		0.18		30		-27		
ii	30		0.17		28		-28		
	38	34 ($\pm$ 3)	0.2	0.197 ($\pm$ 0.025)	45	40 ($\pm$ 11)	-24	-24 ($\pm$ 4)	9
	34		0.22		48		-20		
iii	52		0.22		56		-30		
	46	49 ($\pm$ 3)	0.18	0.203 ($\pm$ 0.021)	66	64 ($\pm$ 8)	-35	-32 ($\pm$ 3)	24
	49		0.21		70		-32		
iv	58		0.32		69		-15		
	61	59 ($\pm$ 1)	0.18	0.233 ($\pm$ 0.077)	67	70 ($\pm$ 3)	-27	-22 ($\pm$ 6)	16
	58		0.2		73		-24		
v	76		0.31		61		-28		
	69	67 ($\pm$ 11)	0.3	0.267 ($\pm$ 0.067)	257	133 ($\pm$ 108)	-19	-23 ($\pm$ 5)	50
	56		0.18		82		-22		
vi	84		0.34		215		-35		
	65	79 ($\pm$ 13)	0.26	0.283 ($\pm$ 0.049)	171	158 ($\pm$ 65)	-38	-39 ($\pm$ 4)	50
	89		0.25		87		-43		
vii	87		0.22		280		-26		
	102	95 ($\pm$ 11)	0.23	0.225 ($\pm$ 0.007)	112	228 ($\pm$ 100)	-32	-29 ($\pm$ 4)	58
	–		–		–		–		
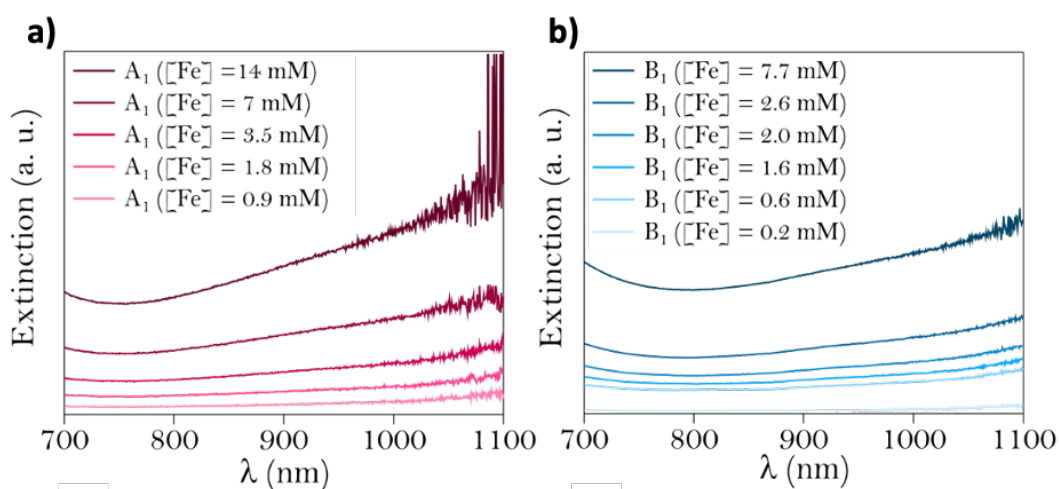
Figure S2. Experimental absorbance at 808 nm and 1064 nm and its dependence on total iron concentration for: a) IONFs (A1) and b) IONF@PS-b-PAA (B1) magnetic micelles
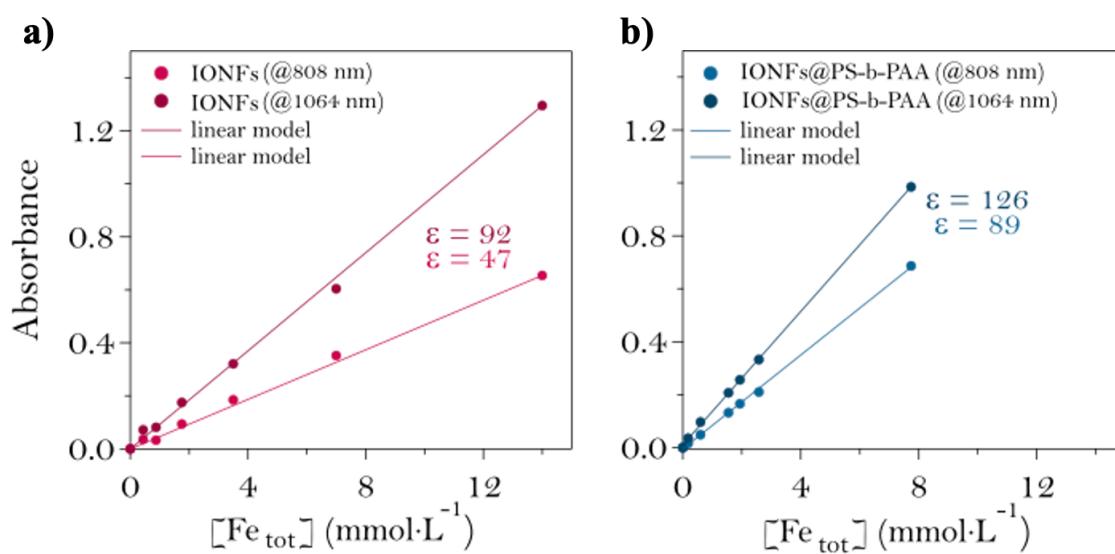

Figure S3. Characterization of the properties of the IONFs and IONFs@PS-b-PAA magnetic micelles. Beer-Lambert plot at two lasers wavelengths 808 nm and 1064 nm of a) IONFs and b) IONFs@PS-b-PAA.

Table S3. Real (n) and imaginary (k) parts of refractive index of Fe_3O_4 for wavelengths ranging from 0.25 µm to 2 µm.

n	k	λ	n	k	λ	n	k	λ	n	k	λ
		µm			µm			µm			µm
1.315	1.899	0.25	0.034	2.99	0.69	0.011	2.739	1.13	0.02	2.681	1.57
1.317	2.007	0.26	0.031	2.972	0.7	0.01	2.737	1.14	0.02	2.68	1.58
1.3	2.11	0.27	0.028	2.956	0.71	0.01	2.734	1.15	0.021	2.679	1.59
1.27	2.197	0.28	0.026	2.942	0.72	0.009	2.732	1.16	0.022	2.678	1.6
1.233	2.261	0.29	0.024	2.929	0.73	0.009	2.729	1.17	0.023	2.677	1.61
1.208	2.307	0.3	0.022	2.916	0.74	0.01	2.727	1.18	0.023	2.677	1.62
1.195	2.357	0.31	0.021	2.903	0.75	0.01	2.725	1.19	0.024	2.677	1.63
1.169	2.416	0.32	0.02	2.892	0.76	0.011	2.723	1.2	0.024	2.677	1.64
1.122	2.454	0.33	0.02	2.882	0.77	0.011	2.721	1.21	0.024	2.677	1.65
1.085	2.45	0.34	0.019	2.872	0.78	0.011	2.719	1.22	0.024	2.676	1.66
1.093	2.43	0.35	0.019	2.862	0.79	0.011	2.718	1.23	0.024	2.676	1.67
1.14	2.433	0.36	0.02	2.853	0.8	0.011	2.716	1.24	0.024	2.676	1.68
1.202	2.47	0.37	0.022	2.845	0.81	0.011	2.715	1.25	0.024	2.675	1.69
1.258	2.545	0.38	0.024	2.838	0.82	0.011	2.714	1.26	0.024	2.674	1.7
1.291	2.645	0.39	0.025	2.833	0.83	0.01	2.712	1.27	0.024	2.674	1.71
1.294	2.756	0.4	0.026	2.828	0.84	0.01	2.709	1.28	0.025	2.673	1.72
1.271	2.863	0.41	0.027	2.824	0.85	0.011	2.708	1.29	0.025	2.673	1.73
1.231	2.962	0.42	0.027	2.82	0.86	0.012	2.706	1.3	0.025	2.673	1.74
1.173	3.052	0.43	0.026	2.816	0.87	0.013	2.705	1.31	0.025	2.672	1.75
1.101	3.126	0.44	0.026	2.813	0.88	0.013	2.704	1.32	0.025	2.672	1.76
1.02	3.181	0.45	0.026	2.809	0.89	0.013	2.703	1.33	0.026	2.671	1.77
0.943	3.217	0.46	0.024	2.805	0.9	0.013	2.702	1.34	0.026	2.672	1.78
0.874	3.242	0.47	0.024	2.801	0.91	0.013	2.7	1.35	0.025	2.671	1.79
0.809	3.264	0.48	0.023	2.798	0.92	0.013	2.699	1.36	0.024	2.67	1.8
0.741	3.28	0.49	0.023	2.794	0.93	0.013	2.697	1.37	0.025	2.669	1.81
0.675	3.282	0.5	0.023	2.791	0.94	0.014	2.696	1.38	0.025	2.668	1.82
0.622	3.272	0.51	0.022	2.789	0.95	0.015	2.695	1.39	0.026	2.667	1.83
0.587	3.262	0.52	0.021	2.787	0.96	0.015	2.693	1.4	0.026	2.666	1.84
0.564	3.266	0.53	0.02	2.784	0.97	0.016	2.693	1.41	0.027	2.665	1.85
0.538	3.286	0.54	0.018	2.781	0.98	0.017	2.692	1.42	0.029	2.664	1.86
0.498	3.318	0.55	0.017	2.778	0.99	0.017	2.692	1.43	0.031	2.664	1.87
0.437	3.348	0.56	0.015	2.775	1.00	0.017	2.691	1.44	0.032	2.665	1.88
0.357	3.361	0.57	0.015	2.771	1.01	0.017	2.69	1.45	0.032	2.666	1.89
0.274	3.348	0.58	0.014	2.768	1.02	0.017	2.689	1.46	0.032	2.667	1.9
0.202	3.312	0.59	0.013	2.765	1.03	0.017	2.687	1.47	0.032	2.667	1.91
0.149	3.265	0.6	0.012	2.762	1.04	0.018	2.686	1.48	0.032	2.667	1.92
0.114	3.218	0.61	0.011	2.759	1.05	0.018	2.686	1.49	0.032	2.667	1.93
0.089	3.175	0.62	0.011	2.755	1.06	0.019	2.685	1.5	0.032	2.667	1.94
0.073	3.135	0.63	0.011	2.753	1.07	0.019	2.684	1.51	0.031	2.667	1.95
0.065	3.102	0.64	0.011	2.75	1.08	0.019	2.683	1.52	0.031	2.667	1.96
0.057	3.074	0.65	0.011	2.747	1.09	0.02	2.683	1.53	0.031	2.666	1.97
0.051	3.051	0.66	0.011	2.745	1.1	0.021	2.682	1.54	0.031	2.666	1.98
0.043	3.029	0.67	0.011	2.742	1.11	0.021	2.682	1.55	0.031	2.665	1.99

Table S4. Real (n) and imaginary (k) parts of refractive index of polystyrene for wavelengths ranging from 0.25 µm to 2 µm.

n	k ($\cdot 10^{-7}$)	λ (µm)	n	k ($\cdot 10^{-7}$)	λ (µm)	n	k ($\cdot 10^{-7}$)	λ (µm)	n	k ($\cdot 10^{-7}$)	λ (µm)
1,62552	8,13	0,4	1,57637	5,55	0,81	1,56707	40,3	1,22	1,56402	192	1,63
1,62163	7,28	0,41	1,57618	4,48	0,82	1,56707	27,9	1,23	1,56432	268	1,64
1,61834	6,82	0,42	1,5758	4,21	0,83	1,56665	20,6	1,24	1,56402	242	1,65
1,61546	6,7	0,43	1,57563	5,34	0,84	1,56688	16,8	1,25	1,56391	387	1,66
1,61279	6,5	0,44	1,57539	5,11	0,85	1,56667	16,6	1,26	1,56342	1050	1,67
1,61037	6,33	0,45	1,57513	5,29	0,86	1,56692	18,8	1,27	1,56376	1600	1,68
1,60797	6,12	0,46	1,57489	12,2	0,87	1,56712	12,7	1,28	1,5636	1370	1,69
1,60594	6,02	0,47	1,57451	9,11	0,88	1,56643	12,7	1,29	1,56341	846	1,7
1,60372	6,09	0,48	1,57437	8,2	0,89	1,56571	15,1	1,3	1,56341	542	1,71
1,60201	6,25	0,49	1,57409	5,35	0,9	1,56643	14,3	1,31	1,56363	480	1,72
1,60021	6,11	0,5	1,57387	4,93	0,91	1,566	15,7	1,32	1,5639	440	1,73
1,59862	6,12	0,51	1,57362	3,93	0,92	1,56583	17,4	1,33	1,56383	273	1,74
1,59721	5,72	0,52	1,57343	2,85	0,93	1,56593	20,3	1,34	1,56336	334	1,75
1,59587	5,62	0,53	1,57315	8,16	0,94	1,56618	22,8	1,35	1,56349	417	1,76
1,59443	5,7	0,54	1,57292	4	0,95	1,56572	20,5	1,36	1,56337	362	1,77
1,59338	5,78	0,55	1,57285	4,71	0,96	1,56639	35,5	1,37	1,56328	272	1,78
1,59217	6,07	0,56	1,57256	2,04	0,97	1,56551	40	1,38	1,56336	306	1,79
1,59084	5,86	0,57	1,57231	2,34	0,98	1,56555	47,8	1,39	1,56314	291	1,8
1,58996	5,95	0,58	1,57216	4,34	0,99	1,56579	50,5	1,4	1,56316	297	1,81
1,58898	5,83	0,59	1,57211	3,49	1	1,56531	57,6	1,41	1,56293	272	1,82
1,5882	6,36	0,6	1,57197	7,34	1,01	1,56534	61,2	1,42	1,56309	244	1,83
1,58734	6,31	0,61	1,57197	7,39	1,02	1,56508	52,4	1,43	1,56296	248	1,84
1,58653	5,93	0,62	1,56996	10,1	1,03	1,5651	50,8	1,44	1,56285	256	1,85
1,58554	6,14	0,63	1,57013	9,61	1,04	1,56522	44,9	1,45	1,56279	268	1,86
1,58493	6,27	0,64	1,5699	9,82	1,05	1,56532	40,1	1,46	1,5632	246	1,87
1,58426	5,83	0,65	1,56958	9,36	1,06	1,56522	40	1,47	1,56337	218	1,88
1,58359	5,86	0,66	1,56904	9,04	1,07	1,5651	46,5	1,48	1,56296	214	1,89
1,583	5,73	0,67	1,56938	8,95	1,08	1,56533	32,3	1,49	1,56302	211	1,9
1,58237	5,64	0,68	1,56916	12,5	1,09	1,56463	30,6	1,5	1,5631	214	1,91
1,5818	5,82	0,69	1,56904	11	1,1	1,56471	28,2	1,51	1,5627	197	1,92
1,58128	5,64	0,7	1,56911	13,5	1,11	1,56419	26,4	1,52	1,56293	189	1,93
1,58061	6,02	0,71	1,56854	18,8	1,12	1,56448	24,5	1,53	1,56262	185	1,94
1,58022	5,55	0,72	1,5687	41,2	1,13	1,56478	22,5	1,54	1,56275	192	1,95
1,57972	5,76	0,73	1,56779	113	1,14	1,56484	18,9	1,55	1,56273	184	1,96
1,57926	5,67	0,74	1,56805	114	1,15	1,56451	19,6	1,56	1,56303	179	1,97
1,57889	5,51	0,75	1,56801	45,2	1,16	1,56462	21,3	1,57	1,56332	179	1,98
1,57821	5,98	0,76	1,56851	29,6	1,17	1,56449	24,1	1,58	1,56277	175	1,99
1,5777	6,08	0,77	1,56822	24,5	1,18	1,56403	28,4	1,59	1,56256	176	2
1,57746	5,46	0,78	1,56803	34,4	1,19	1,56384	33,2	1,6			
1,57703	5,45	0,79	1,56767	46	1,2	1,56384	44,6	1,61			
1,57674	5,54	0,8	1,56757	52,4	1,21	1,56447	81,1	1,62			
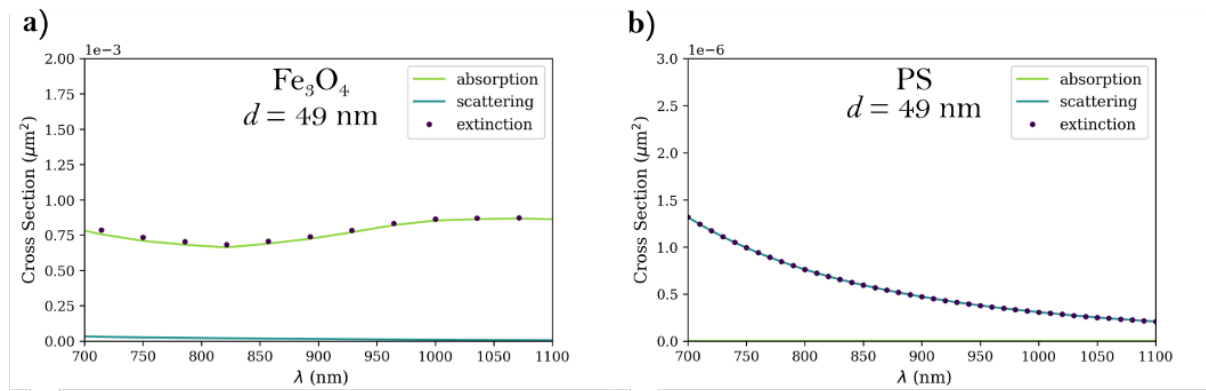
Figure S4. Simulated cross sections as a function of wavelength for a) IONFs and b) PS NPs with a d_{TEM} = 49 nm. Green line: absorption contribution; light blue line: scattering con
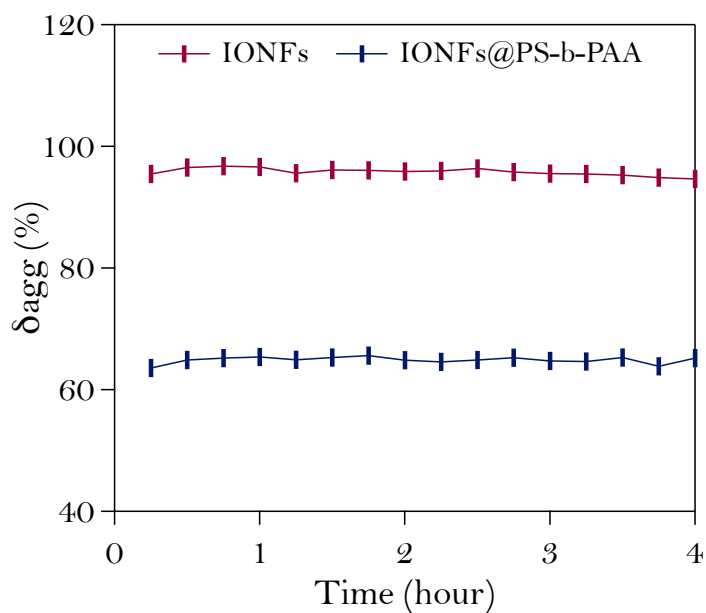
Figure S5. Percentage of aggregation reported as a function of incubation time (at 37°C in complete DMEM) for IONFs at 0.05 mM and IONFs@PS-b-PAA at 0.5 mM